The ACA10 Ca^{2+}-ATPase Regulates Adult Vegetative Development and Inflorescence Architecture in Arabidopsis[1][W][OA]

Lynn George[2], Shawn M. Romanowsky, Jeffrey F. Harper, and Robert A. Sharrock*

Department of Plant Sciences and Plant Pathology, Montana State University, Bozeman, Montana 59717 (L.G., R.A.S.); and Department of Biochemistry, University of Nevada, Reno, Nevada 89557 (S.M.R., J.F.H.)

The Arabidopsis (*Arabidopsis thaliana*) *compact inflorescence* (*cif*) genotype causes altered adult vegetative development and a reduction in elongation of inflorescence internodes resulting in formation of floral clusters. The *cif* trait requires both a recessive mutation, *cif1*, and the activity of a naturally occurring dominant allele of an unlinked gene, $CIF2^D$. We show here that the *pseudoverticillata* mutation is allelic with *cif1* and that the product of the *CIF1* gene is ACA10, a member of the large family of P-type Ca^{2+}-ATPases found in higher plants. T-DNA insertion mutations in *ACA10*, but not in the two other Arabidopsis plasma membrane Ca^{2+}-ATPase-encoding genes, *ACA8* and *ACA9*, cause a *cif* phenotype when combined with the dominant $CIF2^D$ modifier allele. Therefore, *ACA10* has a unique function in regulating adult phase growth and inflorescence development. The wild-type *ACA8* and *ACA10* mRNAs are present at similar levels, and the two promoter-β-glucuronidase fusion transgenes show very similar expression patterns. Moreover, transformation of the *cif* mutant with an extra copy of the *ACA8* gene, which causes overexpression of the *ACA8* transcript, can complement the *cif* phenotype. This suggests that these two Ca^{2+} pump genes have distinct but related activities and that their differential functions can be altered by relatively small changes in their patterns or levels of expression. The correspondence between *cif1* and mutations in *ACA10* establishes a genetic link between calcium transport, vegetative phase change, and inflorescence architecture.

Regulatory pathways that control cell growth and division in response to developmental transitions are critical to producing the often conspicuous structural changes that occur as plants progress through their life cycles. Development of the plant shoot results from activity of the shoot apical meristem (SAM), a highly organized group of dividing and differentiating cells at the shoot tip, and occurs by reiterative formation of phytomers, which consist of a node bearing a lateral organ, such as a leaf, a stem segment, or internode, and one or more axillary meristems. The activities of meristems, the determinacy or indeterminacy of those groups of cells, and the patterning and expansion growth of individual organs determine plant architectures (Sussex and Kerk, 2001; McSteen and Leyser, 2005). Internode elongation is often an important developmentally controlled component of plant architecture. For example, vegetative growth in Arabidopsis (*Arabidopsis thaliana*), which is characterized by production of large leaves and repressed axillary meristem development, is accompanied by little or no internode elongation and results in formation of a compact rosette. At the initiation of flowering, conversion of the SAM to an inflorescence meristem derepresses axillary meristem outgrowth and activates extensive internode elongation, resulting in an aerial branched inflorescence architecture. Variation in the number and pattern of plant inflorescence branches and in the elongation of inflorescence internodes produces much of the diversity of inflorescence morphologies observed in flowering plants (Weberling, 1989).

Development of the postembryonic plant shoot occurs in three phases: juvenile vegetative, adult vegetative, and reproductive (Poethig, 2003). Juvenile and adult vegetative identities are characterized by the absence and presence, respectively, of competence to initiate reproductive phase and, in Arabidopsis, by distinctive rosette leaf morphologies (Telfer et al., 1997). Reproductive phase is characterized by production of flowers and formation of a branched elongated inflorescence. Several Arabidopsis genes have been implicated in control of internode growth, based largely upon their effects on elongation of the inflorescence. Loss-of-function mutations in the *ERECTA* (*ER*) gene result in reduced inflorescence internode elongation and shortened aerial organs, including flowers, pedicels, and siliques (Torii et al., 1996). *ER* encodes an Leu-rich repeat-receptor-like kinase that is

[1] This work was supported by the National Research Initiative of the U.S. Department of Agriculture (grant no. 2004–35304–14933 to R.A.S.), by the Department of Energy (grant no. DE–FG03–94ER20152 to S.M.R. and J.F.H.), and by the National Institutes for Health (grant no. GM070813–01).

[2] Present address: Department of Cell Biology and Neurosciences, Montana State University, Bozeman, MT 59717.

* Corresponding author; e-mail sharrock@montana.edu.

The author responsible for distribution of materials integral to the findings presented in this article in accordance with the policy described in the Instructions for Authors (www.plantphysiol.org) is: Robert A. Sharrock (sharrock@montana.edu).

[W] The online version of this article contains Web-only data.

[OA] Open Access articles can be viewed online without a subscription.

www.plantphysiol.org/cgi/doi/10.1104/pp.107.108118

highly expressed in the SAM and in developing lateral organs (Yokoyama et al., 1998). *BREVIPEDICELLUS* and *PENNYWISE* encode, respectively, KNOTTED1-like (KNOX) and BEL1-like (BELL) homeobox proteins that physically interact with each other, show a synergistic effect on inflorescence internode patterning and elongation, and are expressed in a discrete domain of the inflorescence meristem (Douglas et al., 2002; Venglat et al., 2002; Smith and Hake, 2003; Bhatt et al., 2004; Kanrar et al., 2006). *ACAULIS5*, one of two Arabidopsis spermine synthase genes, is highly expressed in stem internodes, and loss-of-function mutations in this gene result in dramatically shortened inflorescence internodes and premature arrest of the inflorescence meristem (Hanzawa et al., 1997, 2000). The extent to which these different genes and gene products interact with each other in regulating stem elongation growth has not been extensively assessed, although a wild-type *ER* gene partially suppresses the *bp* phenotype (Douglas et al., 2002).

The Arabidopsis *compact inflorescence* (*cif*) mutant shows a severe lack of elongation of inflorescence internodes, resulting in the formation of tightly bunched clusters of flowers either at the ends of very short inflorescence shoots or within the center of the rosette (Goosey and Sharrock, 2001). The mutant phenotype includes slight reductions in elongation of pedicels and expansion of cauline leaves, but floral development is normal. Under most growth conditions, vegetative development of *cif* is indistinguishable from the wild type. However, when grown under long days of fluorescent light, the adult vegetative leaves, but not the juvenile leaves, of the *cif* rosette show markedly reduced expansion. This suggests that regulatory pathways involving the *CIF* genes are activated at the juvenile to adult vegetative phase change and function to control cell division and expansion from that phase transition up to the point of floral meristem development. The *cif* phenotype is inherited as a two-gene trait requiring homozygosity for a recessive allele, *cif1*, and either heterozygosity or homozygosity for a naturally occurring dominant modifier gene, $CIF2^{D}$ (Goosey and Sharrock, 2001). We describe here the identification of the *CIF1* gene as *ACA10*, a gene encoding a P-type IIB Ca^{2+}-ATPase. This finding suggests that regulation of internode elongation in response to phase change is mediated at least in part via calcium signaling and that this requires the activity of a specific member of the Ca^{2+}-ATPase family.

Calcium is a ubiquitous second messenger in eukaryotic signal transduction cascades. In plants, Ca^{2+}-binding proteins in the cytoplasm and nucleus, such as calmodulin, calcineurin B-like proteins, and Ca^{2+}-dependent protein kinases (CDPKs), act as sensors and transduce specific calcium signatures into downstream effects. Intracellular Ca^{2+} levels have been shown to be modulated in response to hormones, light, mechanical disturbances, abiotic stress, and pathogen elicitors (White and Broadley, 2003). Growing evidence indicates that Ca^{2+} signals can be propagated as waves of Ca^{2+} release and uptake and that specific information is encoded in the amplitude and frequency of these oscillations within the cytosol (Evans et al., 2001; Sanders et al., 2002). Cytosolic Ca^{2+} homeostasis and the characteristics of perturbations, such as Ca^{2+} spikes or oscillations, are controlled by both influx pathways, principally involving the activities of Ca^{2+} channels, and efflux pathways in which Ca^{2+}-ATPase pumps and Ca^{2+} exchangers remove cytosolic Ca^{2+} to storage sites within and outside the cell (Sanders et al., 2002; Berridge et al., 2003; Hetherington and Brownlee, 2004). The relative importance of the high-affinity Ca^{2+} pumps and the lower affinity H^{+}/Ca^{2+} exchangers in merely maintaining intracellular Ca^{2+} homeostasis versus actively influencing the spatial and temporal aspects of Ca^{2+} perturbations is not known.

Fourteen genes encode P-type Ca^{2+}-ATPases in Arabidopsis (Baxter et al., 2003). Four of these encode type IIA or ER-type Ca^{2+}-ATPase (ECA) pumps and 10 encode type IIB or autoinhibited Ca^{2+}-ATPase (ACA) pumps. The ACA ATPases contain N-terminal calmodulin-binding domains and can be activated through binding of Ca^{2+}/calmodulin or inhibited, at least in some cases, through phosphorylation by CDPKs (Harper et al., 1998; Hwang et al., 2000b). The ACA proteins cluster into four related groups based upon sequence similarity (Baxter et al., 2003), and members of these clusters localize to different cellular membranes (Huang et al., 1993; Harper et al., 1998; Bonza et al., 2000; Geisler et al., 2000). ACA8 and ACA9 have been shown to localize predominantly to the plasma membrane (Bonza et al., 2000; Schiott et al., 2004). The function of only one of the P-type Ca^{2+}-ATPases is known; mutations in the *ACA9* gene cause defects in pollen tube growth and partial male sterility (Schiott et al., 2004). Here, we present evidence that the recessive *cif1* mutations are lesions in the *ACA10* gene. In addition, we show that mutations in the highly related *ACA8* and *ACA9* genes do not cause *cif* phenotypes when combined with the dominant $CIF2^{D}$ modifier allele. This demonstrates a unique function for the ACA10 Ca^{2+} pump in regulating plant elongation growth during the adult vegetative growth phase and in determining key aspects of inflorescence structure.

RESULTS

The *cif1* Mutation Is Associated with a Region of Reduced Recombination

The *cif* mutant, although not T-DNA tagged, was identified among the progeny of a T-DNA transformation. The *cif* phenotype results from a recessive mutation, *cif1*, and a dominant modifier gene, $CIF2^{D}$, the required allele of which is present in the Nossen (No-0; $CIF2^{D:No\text{-}0}$) but not the Columbia (Col; $CIF2^{Col}$) genetic background. In preliminary mapping experiments, the *CIF1* and *CIF2* genes were localized to the

two ends of chromosome 1 (Goosey and Sharrock, 2001). However, further mapping showed that the recessive locus, *cif1*, is linked to a region on chromosome 1 that shows strongly suppressed recombination (L. George and R.A. Sharrock, unpublished data), suggesting that the *cif1* mutation is associated with a chromosomal rearrangement. Consistent with this, *cif1*/*CIF1* heterozygous plants show approximately 50% reduced pollen viability (Supplemental Fig. S1).

pseudoverticillata Is an Allele of *cif1* and Requires the Activity of a $CIF2^D$ Modifier Allele

The Arabidopsis *pseudoverticillata* (*psv*) mutant, which was isolated in a screen for methyl nitrosourea-induced morphological mutants in the ecotype S96, was described as having a clustered inflorescence (Relichova, 1976). Figure 1A shows that the *cif* and *psv* mutants produce very similar floral cluster phenotypes. Progeny of a No-0 *cif* × S96 *psv* cross show no complementation of the mutant phenotype in either the F_1 or the F_2 generation. In addition, F_2 progeny of a S96 *psv* × Col wild type cross segregate the *psv* trait in a 3:16 ratio (93:520; $P = 0.3$), and recombinant frequency mapping among these F_2 progeny shows that a dominant gene ($CIF2^{D:S96}$), linked to the same chromosome 1 markers as the dominant $CIF2^{D:No\text{-}0}$ gene, is required for expression of the *psv* trait. Therefore, the *cif* and *psv* mutants represent independent recessive mutations in the same *CIF1* gene that require the activity of naturally occurring dominant alleles of the same unlinked *CIF2* modifier gene. The mutant plant lines and the recessive alleles corresponding to the *cif* and *psv* mutant phenotypes have been designated *cif1-1* and *cif1-2*, respectively, and the dominant alleles $CIF2^{D:No\text{-}0}$ and $CIF2^{D:S96}$. It is possible that $CIF2^{D:No\text{-}0}$ and $CIF2^{D:S96}$ are the same naturally occurring *CIF2* gene allele.

The *cif* Mutants Contain Mutations in the *ACA10* Ca^{2+}-ATPase Gene

F_2 progeny of the S96 *cif1-2* × Col wild type cross were analyzed for segregation of the recessive *cif1* and dominant $CIF2^D$ alleles as described previously for the No-0 *cif1-1* × Col wild type cross (Goosey and Sharrock, 2001). Unlike the recessive *cif1-1* mutation, which showed linkage to markers at the bottom of chromosome 1, the *cif1-2* mutation showed linkage to markers on the top arm of chromosome 4. Subsequent reanalysis of the original No-0 *cif1-1* × Col mapping population using these chromosome 4 markers showed tight linkage of these chromosome 4 sequences to both the *cif* phenotype and also to chromosome 1 molecular markers. These anomalous linkage relationships were not observed in crosses of No-0 wild type to Col or ecotype Landsberg *erecta* (L*er*) wild type. These data are consistent with the interpretation that the original recessive *cif1-1* mutation is associated with a translocation between chromosomes 1 and 4 and that the wild-type *CIF1* gene is in fact located on the top arm of chromosome 4. A parental mapping line homozygous for the dominant $CIF2^{D:S96}$ allele and heterozygous for the recessive *cif1-2* allele was constructed, and analysis of 1,000 recombinant F_2 chromosomes delimited the *cif1-2* allele to an 80-kb region of chromosome 4. Candidate genes from the 80-kb interval were sequenced and mutations in the *ACA10* Ca^{2+}-ATPase gene were identified in both the No-0 *cif1-1* and S96 *cif1-2* mutants. The *ACA10* gene contains 33 introns, and, as shown in Figure 2A, the *cif1-1* mutant was found to have a 23-bp deletion in the exon sequence immediately following intron number 28. No evidence of a translocation breakpoint in this region was observed, indicating that the 23-bp deletion and the translocation are distinct but genetically linked mutations. A single nucleotide G-to-A transition in the first base of intron number 5 of *ACA10* was identified in *cif1-2* (Fig. 2A).

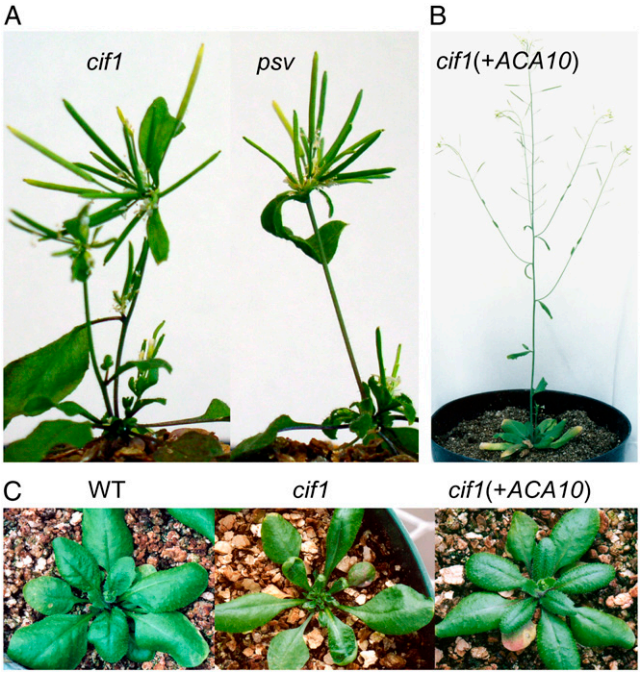

Figure 1. Inflorescence and rosette phenotypes of the *cif1-1* and *cif1-2* (*psv*) mutants and transgenically complemented *cif1-1* plants. Plants were grown under a 16-h photoperiod of fluorescent light. A, The *cif-1* and *psv*/*cif1-2* mutants exhibit similar floral clustering phenotypes. B and C, Transformation of the *cif1-1* mutant with an *ACA10* transgene complements the inflorescence internode elongation phenotype and the adult vegetative leaf expansion phenotype.

The *ACA10* mutations in the *cif1-1* and *cif1-2* mutants are both located at exon/intron boundaries. To test their effects on processing of the *ACA10* pre-mRNA, cDNA samples synthesized from No-0 and S96 wild-type RNA and from *cif1-1* and *cif1-2* RNA were used as templates in reverse transcription (RT)-PCR. Figure 2B shows that primers flanking the region of the *ACA10* gene from exon number 28 to exon number 30 amplify the expected 214-bp product from wild-type or *cif1-2* cDNA, corresponding to correctly

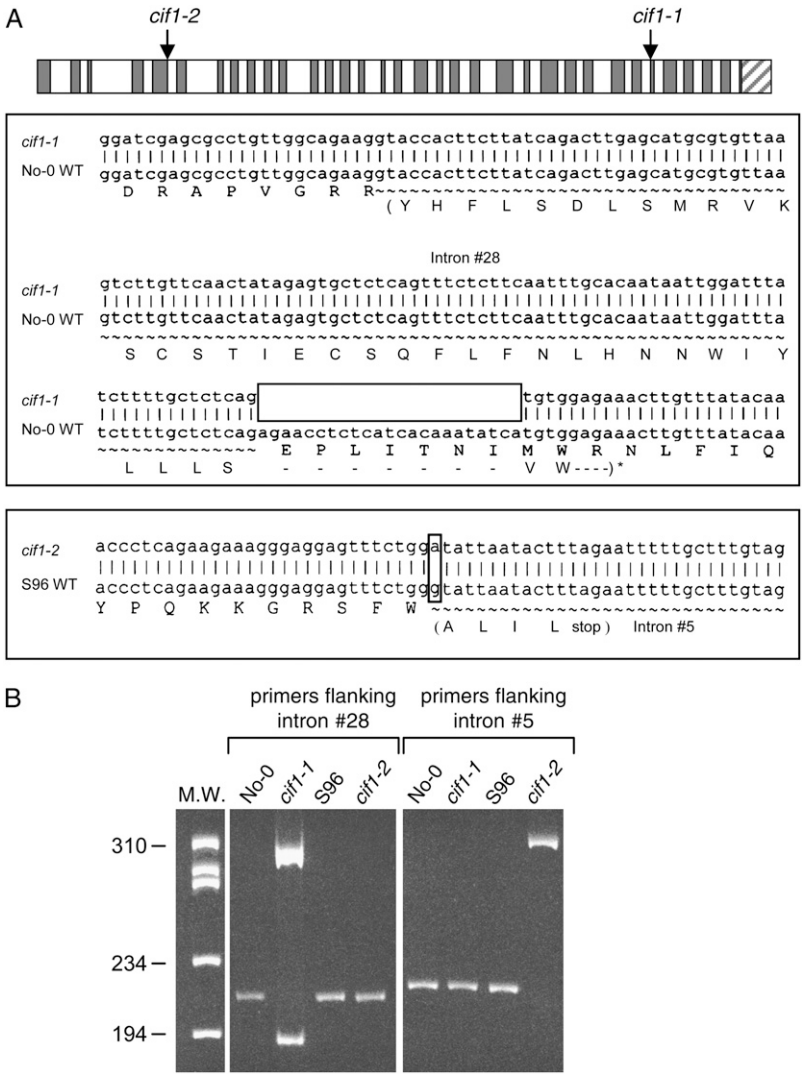

Figure 2. Molecular characterization of the *cif1-1* and *cif1-2* mutations in the *ACA10* gene. A, The locations of the *cif1-1* and *cif1-2* mutations are illustrated on the *ACA10* gene, which contains 34 coding sequence exons and 33 introns. The *cif1-1* mutation is a 23-bp deletion immediately adjacent to the intron number 28 3′ boundary. The *cif1-2* mutation is an A-to-G transition of the first nucleotide of intron number 5. B, Total RNA from *cif1-1* and *cif1-2* mutant seedlings was subjected to RT-PCR analysis of the *ACA10* transcript using primers that flank the *cif1-1* mutation and amplify from exon 28 to exon 30, or primers that flank the *cif1-2* (*psv*) mutation and amplify from exon 5 to exon 6 (see "Materials and Methods").

processed *ACA10* mRNA, but they amplify two bands of altered size from *cif1-1* cDNA. Sequencing of the upper *cif1-1* RT-PCR band shows that it contains the 23-bp deletion and retains the 110-bp intron number 28, producing an insertion/deletion derivative of the ACA10 protein that regains the correct reading frame at Trp-945 (Fig. 2A). Sequencing of the lower *cif1-1* band shows that intron number 28 is correctly processed from this fraction of the *cif1-1* mRNA, but this mRNA contains the 23-bp deletion, which alters the reading frame so that a stop codon is encountered after the inclusion of 32 incorrect residues. Hence, the *cif1-1* allele results in production of some level of both a C-terminally truncated ACA10 protein and an insertion/deletion variant of the protein. Figure 2B shows that primers flanking *ACA10* intron number 5, which contains the point mutation found in *cif1-2* (*psv*), amplify the expected 217-bp product from wild-type or *cif1-1* cDNA, which corresponds to processed *ACA10* mRNA lacking the intron, but they amplify a 324-bp product from *cif1-2* cDNA. This band was sequenced and found to retain intron number 5 with the G-to-A transition as the first base, generating an in-frame stop codon five codons into the intron (Fig. 2A). Therefore, the *cif1-2* mutation is likely an *aca10* null allele.

To confirm the identity of *ACA10* as the *CIF1* gene, a 9.3-kb DNA fragment containing the wild-type allele of *ACA10* was transformed into *cif1-1* plants. Figure 1, B and C, shows that *cif1-1* plants transformed with the *ACA10* transgene have a wild-type phenotype, with normal development of adult vegetative organs, including adult leaves of the rosette and inflorescence internodes.

T-DNA Mutations in *ACA10*, But Not *ACA8* or *ACA9*, Cause a *cif* Phenotype When Combined with the *CIF2*^{D} Modifier Allele

The ACA8, ACA9, and ACA10 Ca^{2+}-ATPases are approximately 70% identical in amino acid sequence and comprise a discrete subfamily within the family of 10 Arabidopsis ACA proteins (Fig. 3A). ACA8 and

ACA9 have previously been shown to localize to the plasma membrane (Bonza et al., 2000; Schiott et al., 2004). T-DNA insertion mutations in the *ACA8*, *ACA9*, and *ACA10* genes were identified in Arabidopsis ecotype Wassilewskija (Ws; Fig. 3B). The location and molecular properties of the *aca9-1* allele have been described previously (Schiott et al., 2004). The *aca10-1* T-DNA is inserted in intron number 17 of the *ACA10*

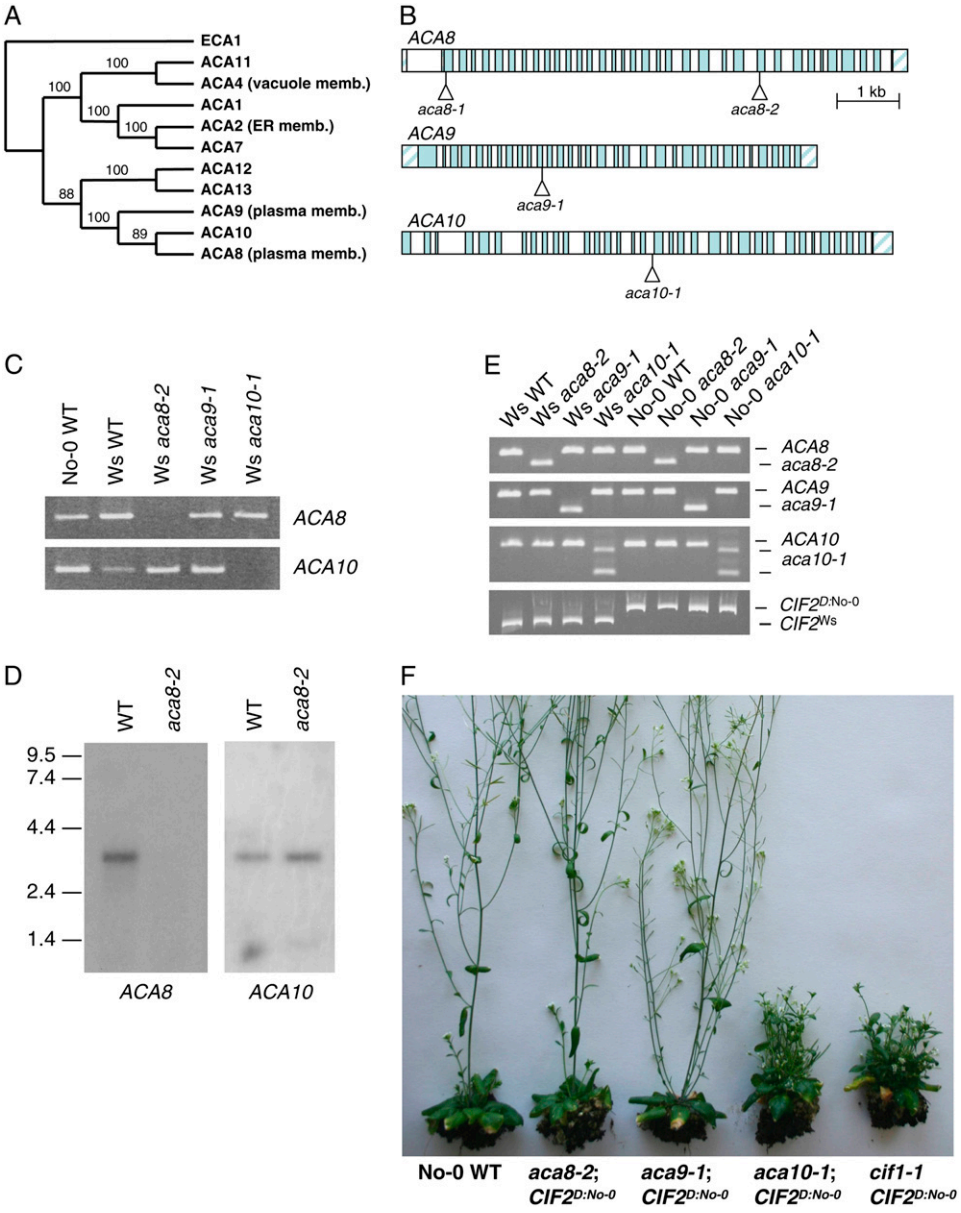

Figure 3. Phenotypic effects of *aca8*, *aca9*, and *aca10* T-DNA insertion mutations when combined with the $CIF2^{D:No-0}$ modifier gene. A, Phylogenetic analysis of the 10 Arabidopsis ACA Ca^{2+}-ATPase protein sequences, with the ECA1 Ca^{2+}-ATPase protein as outgroup, produces a single most parsimonious tree. Bootstrap values from 2,000 replications are shown. B, The locations of T-DNA insertions in the transcribed regions of the *ACA8*, *ACA9*, and *ACA10* genes are indicated. Exons are shown as shaded boxes and introns as unshaded boxes. C, The *aca8-2* and *aca10-1* mutations block transcription downstream of the insertion sites. Total RNA was prepared from seedlings of the original Ws *aca8-2*, *aca9-1*, and *aca10-1* T-DNA lines, and RT-PCR was performed with primers that amplify sequences in the 3′ ends of the *ACA8* and *ACA10* transcripts. D, Blot analysis of poly(A)-selected RNA from wild type and the *aca8-2* mutant probed with gene-specific fragments from the 5′ coding regions of *ACA8* and *ACA10*. E, Genotypes at the T-DNA insertion loci and at the *CIF2* locus were determined for the original lines in the Ws genetic ($CIF2^{Ws}$) background and for representative BCII F_3 lines following introgression of the T-DNA insertions into the No-0 genetic background ($CIF2^{D:No-0}$). DNA of the indicated lines was analyzed by PCR to test for homozygosity for the respective insertion mutation and for the allele state at the *CIF2* modifier gene. F, Representative BCII F_3 plants of the *aca8-2*, *aca9-1*, and *aca10-1* lines containing the $CIF2^{D:No-0}$ allele grown under a 16-h photoperiod of fluorescent light.

gene, with one border at 4,041 bp and the other at 4,067 bp downstream of the start codon. The *aca9-1* and *aca10-1* T-DNA alleles result in lack of expression of their respective transcripts downstream of the insertion sites (Schiott et al., 2004; Fig. 3C). Two *aca8* T-DNA alleles were analyzed: *aca8-1*, which is inserted 35 bp downstream of the ATG in the first coding sequence exon, and *aca8-2*, which is inserted in the 25th coding sequence exon with borders at 5,101 bp and 5,112 bp. In RT-PCR analysis of RNA isolated from the *aca8-1* mutant line, low levels of *ACA8* transcript sequences from downstream of the insertion site were detected (L. George and R.A. Sharrock, unpublished data). This indicates that transcription of the 3′ end of the *ACA8* coding sequence, beginning downstream of nucleotide +35, may occur in this line, perhaps initiated from an internal T-DNA promoter. The *aca8-2* mutation blocks transcription of mRNA sequences downstream of the T-DNA insertion site (Fig. 3C), and RNA-blot analysis confirms the absence of full-length *ACA8* transcript in this line (Fig. 3D). In the experiments described below, both the *aca8-1* and *aca8-2* mutations were analyzed and gave the same results, but only data for the presumptive null *aca8-2* are presented. Table I and Supplemental Figure S2 show that, in the Ws genetic background, the *aca8*, *aca9*, and *aca10* T-DNA mutants all lack an adult phase leaf expansion phenotype, flower at the same time as the wild type, and have raceme inflorescences very similar to Ws wild-type plants.

The *cif1-1* and *cif1-2* mutations are reduction-of-function or loss-of-function *aca10* alleles, so the observation that *aca10* T-DNA mutations do not cause a *cif* phenotype in the Ws background indicates that, like $CIF2^{Col}$ and $CIF2^{Ler}$, $CIF2^{Ws}$ does not function as a dominant modifier gene similar to $CIF2^{D:No\text{-}0}$ and $CIF2^{D:S96}$. It is predicted, therefore, that combining an *aca10* T-DNA mutation with $CIF2^{D:No\text{-}0}$ should result in a *cif* phenotype. To confirm this and to test whether loss of function of either *ACA8* or *ACA9* causes *cif*-like characteristics in combination with the $CIF2^{D:No\text{-}0}$ modifier gene, Ws lines homozygous for the *aca8-1*, *aca8-2*, *aca9-1*, and *aca10-1* T-DNA alleles were crossed to No-0 wild type and then backcrossed twice to No-0 to introgress the T-DNA insertion mutations into the No-0 genetic background. BCII F_1 progeny, heterozygous for the T-DNA allele and homozygous for $CIF2^{D:No\text{-}0}$, were selfed, and the BCII F_2 progeny were scored for their T-DNA insertion genotype and their inflorescence phenotypes. All *aca10-1/aca10-1* $CIF2^{D:No\text{-}0}/CIF2^{D:No\text{-}0}$ F_2 homozygotes derived from these crosses exhibited a *cif* phenotype, including reduced elongation of adult leaves and inflorescence internodes and reduced apical dominance. In contrast, *aca8-1/aca8-1* $CIF2^{D:No\text{-}0}/CIF2^{D:No\text{-}0}$, *aca8-2/aca8-2* $CIF2^{D:No\text{-}0}/CIF2^{D:No\text{-}0}$, and *aca9-1/aca9-1* $CIF2^{D:No\text{-}0}/CIF2^{D:No\text{-}0}$ F_2 segregants showed wild-type adult vegetative and inflorescence development phenotypes. Figure 3, E and F, and Table I present the analysis of representative F_3 progeny from these crosses. These results demonstrate that, among the mutations in these three highly related Ca^{2+} pump genes, only *aca10* loss-of-function alleles interact with the dominant $CIF2^{D}$ modifier allele to produce a *cif* phenotype. As expected from previous studies (Schiott et al., 2004), plants homozygous for the *aca9-1* mutation in the No-0 genetic background show reduced fertility.

Table I. *Inflorescence phenotypes of aca T-DNA mutants and transgenic lines*

Values given are averages of measurements from 6 to 10 individual plants. Values in parentheses are SES of the means. Plants were grown under a 16-h photoperiod of fluorescent light. Internode lengths, total inflorescence lengths, and number of secondary inflorescences were measured on day 45 for the Ws lines and on day 50 for the No-0 lines. The No-0 *aca8-2*, *aca9-1*, and *aca10-1* lines were BCII F_3 plants derived from representative homozygous BCII F_2 parents. The *cif1-1* lines containing chimeric transgenes were T_3 plants derived from representative homozygous T_2 parents. *, $P < 0.05$; **, $P < 0.0001$ (Student's *t* test).

Line	Days to Flower	Average Length of First Six Internodes	Total Length of Inflorescence	No. of 2° Rosette Inflorescences
		mm	*mm*	
Ws wild type	17.6 (0.4)	22.9 (3.4)	364 (9)	4.5 (0.3)
Ws *aca8-2*	17.6 (0.9)	20.9 (2.6)	339 (15)	4.2 (0.4)
Ws *aca9-1*	17.3 (0.7)	24.0 (2.8)	449 (8)*	4.2 (0.6)
Ws *aca10-1*	16.8 (0.8)	25.4 (3.5)	361 (7)	4.0 (0.5)
Ws *aca8-2 aca10-1*	19.0 (0.4)*	21.3 (1.7)	275 (8)**	4.4 (0.4)
No-0 wild type	26.6 (1.0)	23.3 (2.4)	383 (12)	4 (0.3)
No-0 *cif1-1*	27.1 (0.8)	0.94 (0.32)**	7.5 (1.6)**	11.5 (1.1)**
No-0 *aca8-2*	26.6 (1.2)	22.6 (2.2)	382 (9)	5.6 (0.4)*
No-0 *aca9-1*	24.5 (0.8)	21.8 (2.2)	412 (13)	5.2 (0.5)
No-0 *aca10-1*	25.3 (0.6)	4.0 (1.0)**	29 (7)**	12.1 (1.1)**
No-0 wild type	23.7 (0.4)	22.8 (2.4)	315 (16)	5 (0.3)
No-0 *cif1-1*	24.4 (0.4)	1.6 (0.6)**	16 (1.3)**	14.7 (1.5)**
cif1-1 (P_{10}-10)	24.9 (0.4)	22.0 (1.8)	340 (17)	3.5 (0.4)*
cif1-1 (P_{10}-8)	24.2 (0.5)	24.2 (2.7)	398 (41)	4.8 (0.3)
cif1-1 (P_8-10)	25.7 (0.4)*	21.1 (2.1)	363 (30)	3.7 (0.7)
cif1-1 (P_8-8)	24.2 (0.5)	23.1 (2.4)	342 (13)	4.7 (0.3)

The Expression Patterns of the *ACA10* and *ACA8* Genes Are Similar and Are Not Regulated by Growth Phase or the Allele State at *CIF2*

Onset of the *cif* mutant phenotype correlates closely with the juvenile to adult vegetative phase transition (Goosey and Sharrock, 2001). To determine whether this phase change and the onset of the *cif* phenotype also correlate with alteration in the expression of the *ACA10* gene, northern-blot and quantitative RT-PCR (qRT-PCR) analyses were performed on RNA extracted from seedlings and from isolated juvenile and adult leaves of No-0 wild-type and *cif1-1* plants. Figure 4, A and B, shows that the *ACA10* mRNA is present at levels varying less than 2-fold at these stages of vegetative development in both wild-type and mutant plants. Schiott et al. (2004) showed that the *ACA9* transcript is present almost exclusively in pollen and, consistent with this, no signal for the *ACA9* mRNA was detected on RNA blots of vegetative tissues (L. George and R.A. Sharrock, unpublished data). However, northern-blot and qRT-PCR analyses show that, like the *ACA10* mRNA, the *ACA8* mRNA is expressed evenly over the course of seedling, juvenile, and adult vegetative development and at a level very similar to that of the *ACA10* transcript (Fig. 4, A and B).

To further assess the expression patterns of the *ACA10* and *ACA8* genes and the possible effect of the *CIF2* gene or the *cif1* genotype on those patterns, the promoter regions from these genes were transcriptionally fused to the GUS coding sequence and introduced into No-0 wild-type ($CIF2^{D:No\text{-}0}$), Col wild-type ($CIF2^{Col}$), and *cif1-1* mutant plants. Figure 5, A and B, shows that, in No-0 (*ACA10*:GUS) and No-0 (*ACA8*:GUS) lines, both promoters are active throughout roots, leaves, and stems of seedlings and rosette-stage plants, including cotyledons and juvenile and adult rosette leaves. The two promoters also exhibit very similar expression patterns in inflorescences, with strong expression in developing inflorescence internodes, cauline leaves, and flowers (Fig. 5, C–F). Surprisingly, as the inflorescence internodes expand, they exhibit reduced GUS staining, as shown for the *ACA10*:GUS plants in Figure 5, C to E. This is also true for *ACA8*:GUS lines (Fig. 5F). This may reflect dilution of the GUS stain in rapidly expanding cells, as initial RT-PCR analyses of the ACA10 mRNA in dissected inflorescence stems did not show a strong down-regulation of transcript level in those regions (L. George and R.A. Sharrock, unpublished data). The *ACA10*:GUS and *ACA8*:GUS genes were also introduced into Col wild-type and *cif1-1* host plants, and staining patterns very similar to those of the No-0 lines were observed throughout seedling, vegetative, and reproductive growth (L. George and R.A. Sharrock, unpublished data). Therefore, neither the allele state at the *CIF2* gene nor the presence or absence of an *aca10* mutation has a strong effect on these *ACA* promoter expression patterns. In the *cif1-1*(*ACA10*:GUS) and *cif1-1*(*ACA8*:GUS) lines, the one or two elongated inflorescence internodes subtending the floral clusters show low GUS staining, like the elongated internodes of the wild-type lines. However, in the floral clusters, although individual internodes are not distinguishable, the point from which pedicels originate in those clusters stains darkly for GUS activity (Fig. 5G), consistent with relatively strong expression of these genes in unexpanded inflorescence internodes. The expression patterns determined here for the *ACA10* and *ACA8* genes are in agreement with those obtained from microarray data sets presented in Genevestigator (http://www.genevestigator.ethz.ch).

Overexpression of ACA8 Can Complement the *cif1* Mutation

Although the *ACA8* and *ACA10* mRNAs encode related proteins and are expressed in very similar

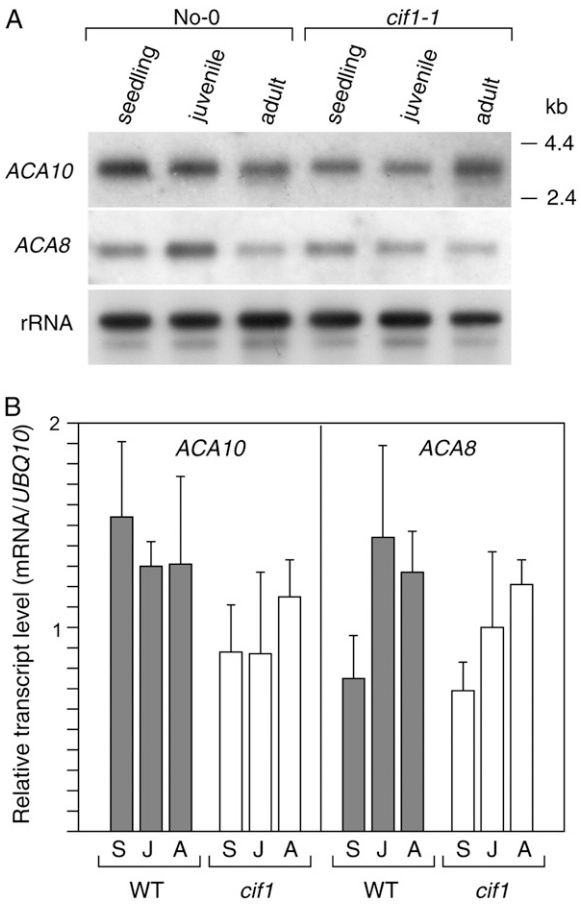

Figure 4. RNA-blot and qRT-PCR analysis of the developmental regulation of the *ACA10* and *ACA8* mRNAs. A, Poly(A)-selected RNA was prepared from seedlings, juvenile rosette leaves, and adult rosette leaves of No-0 wild-type and *cif1-1* plants. Blots were probed with gene-specific probes from the 5′ nonconserved coding regions of the *ACA8* and *ACA10* mRNAs. B, Quantitative RT-PCR analysis was performed on total RNA prepared from the same tissue samples as in part A, above: seedlings (S), juvenile (J), and adult (A) leaves. Error bars represent SDs from the mean values for replicate assays.

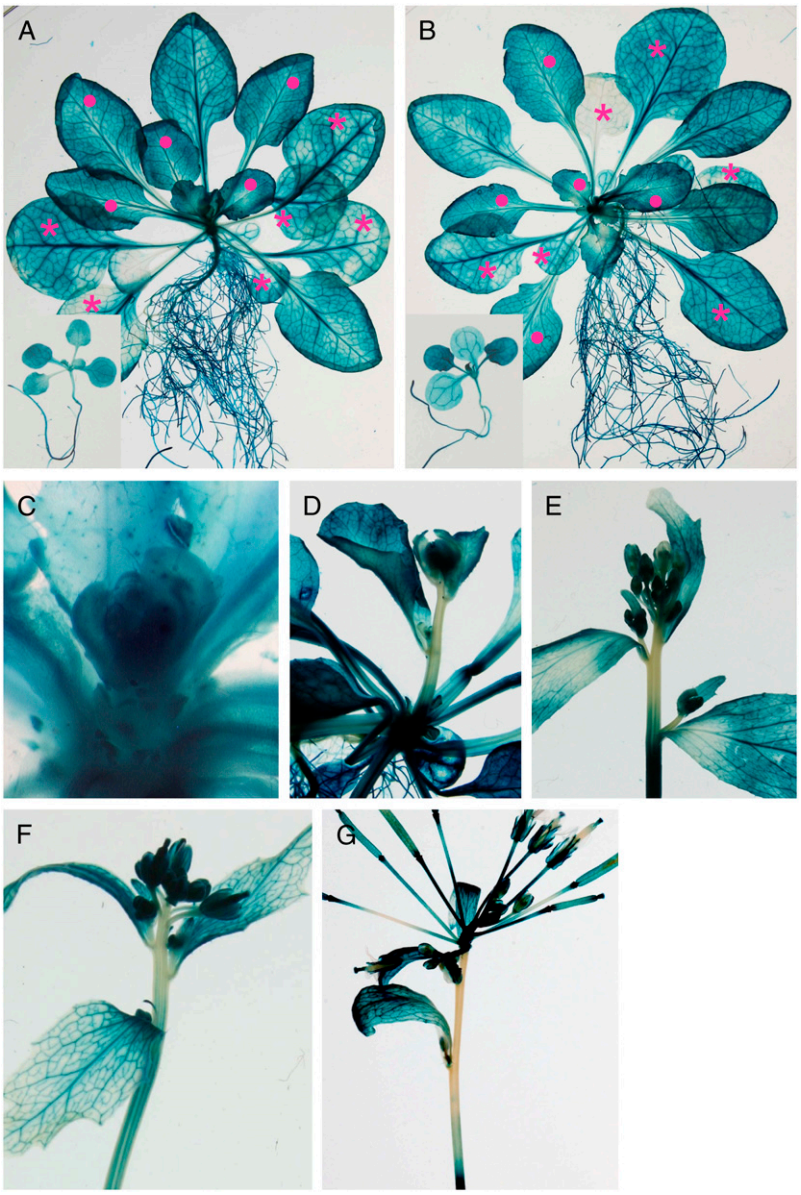

Figure 5. Histochemical analysis of *ACA10*:GUS and *ACA8*:GUS expression patterns. *ACA10*:GUS and *ACA8*:GUS transgenes were introduced into No-0 and Col wild-type plants and into the *cif1-1* mutant. A, Leaf, stem, and root tissues of seedlings (inset) and 28-d-old rosette stage plants of No-0 (*ACA10*:GUS) stain for GUS activity. Leaves with clear juvenile identities in the stained rosettes are labeled with a star and leaves with clear adult identities are labeled with a dot. B, No-0 (*ACA8*:GUS) seedling and rosette expression patterns, as in part A. C to E, Progressive pattern of GUS expression in the developing and elongating primary inflorescence of No-0 (*ACA10*:GUS) plants. F, The primary inflorescence of a No-0 (*ACA8*:GUS) plant shows a similar staining pattern to that of *ACA10*:GUS plants. G, The unexpanded internodes of a *cif1-1*(*ACA10*:GUS) floral cluster stain strongly for GUS activity.

patterns, only *aca10* mutations cause the *cif* phenotype when combined with the $CIF2^{D:No-0}$ modifier gene (Fig. 3D). This suggests either that the two Ca^{2+} pumps have diverged in function at the protein level or that there are aspects of the regulation of the genes, not apparent in RNA quantification or GUS fusion analyses, that underlie their functions. To determine whether the differential functions of *ACA8* and *ACA10* can be specifically attributed to their transcription regulatory regions or to their protein coding regions, transgenes were constructed in which the genomic coding sequences for the ACA8 and ACA10 proteins were fused to the *ACA8* and *ACA10* promoters at their ATG start codons (Fig. 6A). In all cases, the same 5′ upstream promoter sequences were used to make these constructs as the *ACA10*:GUS and *ACA8*:GUS fusion genes analyzed in Figure 5 (see "Materials and Methods"). The P_{10}-10, P_{10}-8, P_8-10, and P_8-8 genes were introduced into *cif1-1* host plants, and multiple independent transgenic lines that segregated as single insertion events in the T_2 generation were isolated for each construct. Figure 6B shows that T_3 lines that are homozygous for the various transgene inserts express the transgene-encoded mRNAs and are not strongly altered in expression of the endogenous *ACA10* and *ACA8* genes. Table I gives flowering time and inflorescence morphology data for representative homozygous T_3 lines containing each construct. As expected, the P_{10}-10 gene complements the *cif1* phenotype in the T_1 and subsequent T_2 and T_3 generations (Table I). The P_{10}-8 transgene also very efficiently complements the *cif* trait, suggesting that, with regard to their capacities to transgenically regulate the *cif* trait, the ACA8 and ACA10 proteins are interchangeable.

This is similar to the observed ability of a P_9-8 transgene to complement the *aca9*-reduced fertility phenotype (Schiott et al., 2004) and confirms that all three of these genes likely encode plasma membrane-localized pumps with similar Ca^{2+}-transporting activities.

Surprisingly, the P_8-10 and P_8-8 transgenes were also found to be capable of complementing the *cif* phenotype in homozygous T_3 lines. Initial T_1 plants carrying these transgenes were observed to be variable for the phenotype, with some elongated inflorescence stems and some floral clusters, but all *cif1-1*(P_8-8) and *cif1-1*(P_8-10) lines bred to homozygosity in the T_2 and T_3 generations were strongly complemented (Table I). This indicates that, when incorporated in transgenes, both the *ACA10* and *ACA8* promoter regions are capable of producing a Ca^{2+}-ATPase expression pattern needed to complement the *cif* phenotype. To further investigate this, the level of total *ACA8* and *ACA10* mRNA present in several of each of the complemented T_3 transgenic lines was determined by qRT-PCR. Figure 6C shows that the P_{10}-10 and P_8-10 lines contain total amounts of *ACA10* transcript, including both the endogenous mutant transcript and the transgene product, which is from 1.5- to 7-fold over that of the control lines. The P_{10}-8 and P_8-8 lines overexpress the *ACA8* mRNA from 6- to 15-fold relative to the endogenous *ACA8* gene. The reason that an increased gene dosage of *ACA8* causes such a disproportionately large increase in the *ACA8* transcript is not known. Nevertheless, it appears that, while the diploid copy of the endogenous *ACA8* gene present in nontransgenic *cif1* lines cannot compensate for loss of the *ACA10* gene, overexpression of *ACA8* in the P_8-8 transgenic lines is sufficient to do so.

It is possible that the ACA8 and ACA10 ATPases differ in their transport activities, the types of complexes they form at the plasma membrane, or their regulation by Ca^{2+}/calmodulin or other mechanisms. Nevertheless, expression of at least one of these two pumps above a threshold level in the membranes of cells of adult leaves and inflorescence stems appears to be sufficient to mediate correct intracellular Ca^{2+} dynamics and *CIF* growth signaling. In a $CIF2^D$ genetic background, *aca10* mutations presumably result in pump levels falling below this threshold, whereas *aca8* mutations do not. This suggests that there may be functional redundancy between the *ACA8* and *ACA10* genes. One hypothesis for the activity of the *CIF2* gene might be that a dominant $CIF2^D$ allele down-regulates expression of the *ACA8* gene in critical cells, resulting in a situation where loss of *ACA10* gene expression triggers the *cif* phenotype. To test this hypothesis and assess the interaction of these two Ca^{2+} pump mutations, *aca8-2 aca10-1* double T-DNA mutants were constructed in the No-0 ($CIF2^D$) background and in the Ws genetic background, which does not carry a dominant $CIF2^D$ allele. The *aca8-2 aca10-1* $CIF2^D$ line has a *cif* inflorescence phenotype similar to the *aca10-1* $CIF2^D$ line (R.A. Sharrock, unpublished data). In contrast, the *aca8-2 aca10-1* $CIF2^{Ws}$ line has a raceme inflorescence with a slightly shorter overall length than wild type but clearly elongated internodes (Table I; Supplemental Fig. S2). Therefore, in a genetic background homozygous for a recessive *CIF2* allele, there is no requirement for either the ACA10 or ACA8 Ca^{2+} pump to mediate *CIF* signaling and functional redundancy of the *ACA8* and *ACA10* genes likely does not explain their respective activities in regulating inflorescence internode elongation.

DISCUSSION

Inflorescence Structure, Calcium Signaling, and the Control of Plant Phase-Regulated Development

Specification of the structure of the inflorescence begins with changes in the developmental potential and activity of the apical meristem triggered at the onset of reproductive phase but depends critically upon subsequent control of expansion and elongation of newly formed organs and stem tissues. Extensive inflorescence internode elongation, along with the production of secondary inflorescence meristems in the axils of cauline leaves, generates the open aerial reproductive architecture of Arabidopsis. The *cif* mutant shows a striking reduction in inflorescence internode elongation, due to both lower cell numbers and reduced cell expansion, resulting in a suppressed bolt and closely clustered bracts and flowers (Goosey and Sharrock, 2001). This mutant architecture is functional and fertile and resembles umbel-like architectures, with pedicels originating from a common point, found in other plant species. It is therefore possible that at least some elements of the *cif* pathway have been targets of selection for diverse inflorescence types during plant evolution. The *cif* mutant phenotype is dependent upon the interaction of a recessive *cif1* mutation and a naturally occurring dominant modifier allele of a second gene, $CIF2^D$. The demonstration here that the CIF*1* gene encodes the ACA10 Ca^{2+} pump suggests that loss of function of a specific Ca^{2+} efflux pump, presumably leading to changes in the activities of one or more Ca^{2+}-signaling pathways, strongly alters reproductive architecture. How such a Ca^{2+}-signaling mechanism may relate to internode elongation regulatory mechanisms involving the ER kinase (Shpak et al., 2004), KNOX/BELL homeobox proteins (Kanrar et al., 2006), or spermine synthase (Hanzawa et al., 2000) is not known. However, it is notable that the mutations that defined the roles of those proteins in inflorescence development were all isolated in the L*er* or the Col genetic background, so no interactions of those pathways with the *CIF2* gene are indicated.

Although the most striking aspect of the *cif* phenotypes is the effect on bolting, under certain light conditions, *cif* leaves with adult phase identities also show reduced elongation and expansion, while *cif* leaves with juvenile identities are completely normal (Goosey and Sharrock, 2001). Therefore, the effects of the *cif* mutant

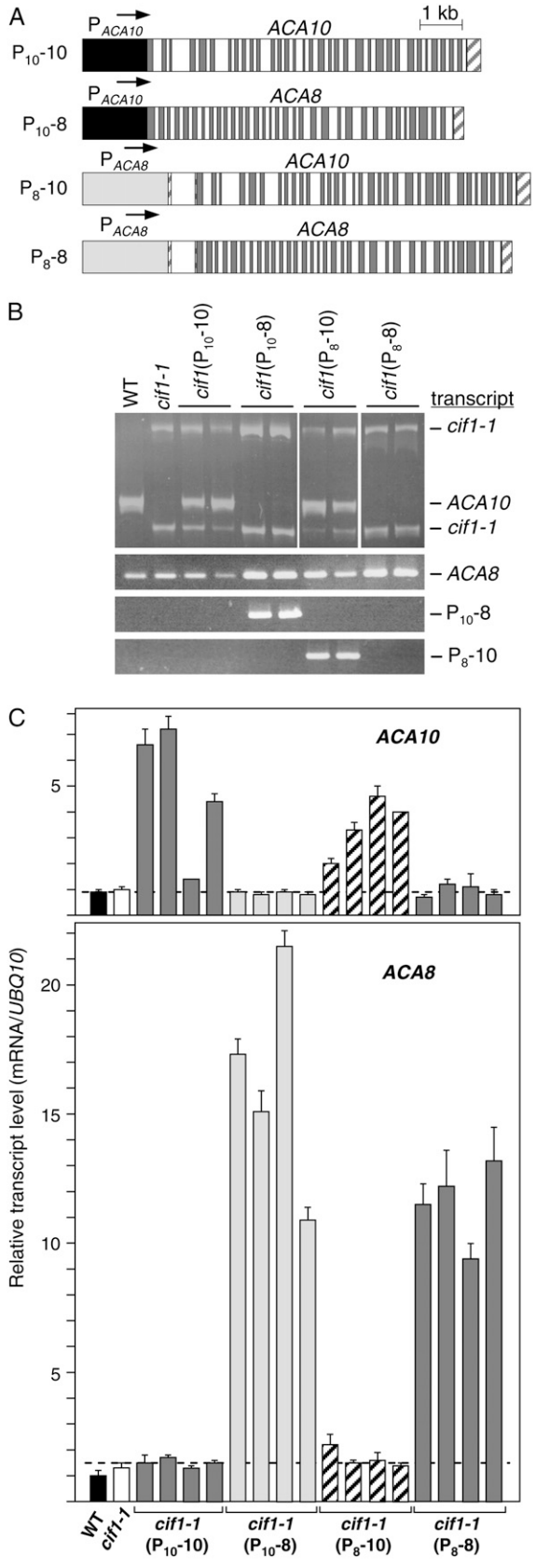

Figure 6. Gene expression analysis of *cif1-1* mutant lines complemented with *ACA8*, *ACA10*, and chimeric transgenes. A, The *ACA10* and *ACA8* promoter regions were fused to the genomic sequences encoding the ACA10 and ACA8 ATPases at their ATG start codons. These transgenes were introduced into the *cif1-1* mutant, and quantitative analysis of the inflorescence phenotypes of representative homozygous T_3 lines are given in Table I. B, Samples of cDNA from homozygous T_3 transgenic lines were assayed for expression of endogenous and transgene-encoded mRNAs by RT-PCR using primer sets that distinguish the wild-type *ACA10* and mutant *cif1-1* mRNAs, detect total *ACA8* mRNA, or detect only the mRNAs produced from the chimeric genes. C, Quantitative PCR was performed to assess the total level of *ACA10* and *ACA8* transcript present in RNA from four independent T_3 transgenic lines for each construct. Dotted lines show the mean of the values for all lines that do not contain a transgene encoding the mRNA being assayed.

genotype first become apparent at the juvenile to adult phase transition. The molecular mechanism that regulates the timing of the juvenile to adult phase transition in Arabidopsis has been shown to involve the activities of small interfering RNAs and microRNAs (Hunter et al., 2006; Wu and Poethig, 2006), but downstream effectors and pathways that mediate morphological changes and developmental responses that are triggered in phase-specific patterns are less well understood. Identification of *CIF1* as the gene encoding the ACA10 Ca^{2+} pump suggests that intracellular Ca^{2+} levels may be an important integration point for such pathways. Analysis of *ACA10* transcript levels and *ACA10*:GUS transgene activity shows that the *ACA10* gene is expressed in many parts of the plant and is not strongly up- or down-regulated at the juvenile to adult phase transition. Moreover, because different plasma membrane Ca^{2+}-ATPase isoforms are expressed in developmentally regulated patterns in animal cells through alternative splicing (Strehler and Zacharias, 2001; Zylinska et al., 2002), we also tested for possible developmentally controlled alternative splicing of the *ACA10* mRNA. RT-PCR analysis of seedling, juvenile leaf, and adult leaf RNA with primers for small sequential fragments covering the entire length of the *ACA10* transcript revealed no evidence for this (L. George and R.A. Sharrock, unpublished data). Therefore, alteration in expression of the *ACA10* gene itself is not currently implicated in the regulation of leaf expansion at the adult phase transition. More likely, adult and reproductive developmental programs, most strikingly inflorescence internode elongation, involve signaling pathways that trigger Ca^{2+} movement across the plasma membrane and, in the absence of the ACA10 pump, the *cif* mutant has abnormal cellular Ca^{2+} dynamics that specifically affect these programs.

Diversity of Regulatory Function among Plant Ca^{2+} Pumps

A family of 14 *ACA* and *ECA* genes encodes Ca^{2+} pumps in Arabidopsis, and different ATPase subfamilies are localized to different cellular membranes (Baxter et al., 2003). The biological activity of only one of these pumps has been previously determined.

T-DNA mutations in the *ACA9* gene were shown to cause defects in pollen cell elongation and, consistent with this, the *ACA9* transcript was shown to be predominantly expressed in pollen (Schiott et al., 2004). Based upon sequence similarity and intron position in their respective genes, the ACA8, ACA9, and ACA10 proteins constitute a well-defined subfamily of Ca^{2+} pumps. We have shown here that, in contrast to *aca9* mutants, *aca8* and *aca10* knockout lines and the *cif1-1* and *cif1-2* lines are unaffected in fertility. Indeed, in the Ws, Col, or L*er* background, no strong effects on the morphology of the plants are seen with any of the *aca10* mutations, and it is only in the presence of the $CIF2^{D}$ modifier allele that reduction of function of this pump results in a strong inflorescence development phenotype. The *aca8* T-DNA mutants show neither reduced fertility nor an effect on inflorescence structure in the presence or absence of the $CIF2^{D}$ modifier allele. Therefore, the functions of these three highly sequence-related Ca^{2+} pumps are divergent. Unlike the *ACA9* mRNA, the *ACA8* and *ACA10* mRNAs are quite strongly expressed in most plant organs over the course of plant development. Recently, the transcription of *ACA8* and *ACA9*, but not *ACA10*, has been shown to be stimulated by abscisic acid (Cerana et al., 2006). The assignment of discrete functions and expression patterns to the *ACA8*, *ACA9*, and *ACA10* genes suggests that a wide array of regulatory Ca^{2+}-signaling pathways in plants may be dependent upon efflux mechanisms involving specific pumps or exchange proteins.

The ACA8 and ACA9 pumps are plasma membrane localized (Bonza et al., 2000; Schiott et al., 2004) and transport Ca^{2+} ions to the apoplast. Although plasma membrane targeting has not been directly shown for ACA10, the observation that the *aca9* and *aca10* mutant phenotypes can be complemented by transgenes containing the *ACA8* coding sequence suggests that these three proteins are very similar in intracellular localization and activity. In addition, all three have protein sequences characteristic of autoregulated ATPases that may be activated through binding of Ca^{2+}/calmodulin (Harper et al., 1998; Geisler et al., 2000; Hwang et al., 2000a). We have shown that introduction of a transgene containing any combination of the *ACA8* or *ACA10* promoters and coding regions can complement the *cif* phenotype. For unknown reasons, these P_{10}-10, P_{10}-8, P_{8}-10, and P_{8}-8 transgenes drive overexpression of the transgene-encoded mRNAs, severalfold higher than the expected gene dosage effect. An *aca8* null mutation does not cause a *cif* phenotype when combined with the dominant $CIF2^{D:No\text{-}0}$ gene, but overexpression of the *ACA8* mRNA is able to complement the *cif* phenotype. It is likely, therefore, that the unique role for ACA10 in regulating reproductive development reflects either subtle differences in the expression patterns or levels of the normal *ACA8* and *ACA10* genes, or differences in the properties of the two pumps themselves relating to their transport activities, autoregulation by Ca^{2+}, or abilities to form membrane complexes with other proteins. However, these differences can be overcome or mitigated by overexpression.

An intriguing aspect of the genetics of the *cif* trait is that the requirement for ACA10 Ca^{2+} pump activity to mediate adult vegetative growth and inflorescence internode elongation is completely dependent upon the allele state of the unlinked *CIF2* gene. Preliminary mapping of *CIF2* shows that it does not correspond to any of the *ACA* Ca^{2+}-ATPase genes (L. George and R.A. Sharrock, unpublished data). At least two alleles of the *CIF2* gene are present in different wild accessions of Arabidopsis. The $CIF2^{D}$ allele present in the No-0 and S96 ecotypes acts in a dominant way in conjunction with *aca10* mutations to alter inflorescence development, whereas the *CIF2* allele found in Col, L*er*, and Ws acts in a recessive manner to suppress the effects of *aca10* mutations. Apparently, dominant $CIF2^{D:No\text{-}0,\ S96}$ alleles predispose the plant to requiring a minimum level of efflux of Ca^{2+} ions by ACA10 in particular cells, whereas recessive $CIF2^{Col,\ Ler,\ Ws}$ alleles obviate the need for that efflux. In a genetic background homozygous for the recessive $CIF2^{Ws}$ allele, even inactivation of both the *ACA8* and *ACA10* genes does not result in a *cif* phenotype. Therefore, the recessive *CIF2* allele effectively disconnects regulation of adult leaf expansion and inflorescence internode elongation from the activities of ACA8 or ACA10. The molecular mechanism for this genetic phenomenon is currently not known, but we have shown that the two different naturally occurring *CIF2* alleles do not strongly influence the pattern or level of *ACA10* or *ACA8* transcription. If the ACA10 and ACA8 pumps are regulated through binding of Ca^{2+}/calmodulin, or through phosphorylation by CDPKs as has been shown for ACA2 (Hwang et al., 2000b), it is possible that *CIF2* encodes a component of a transport regulatory mechanism. The striking inflorescence elongation phenotype elicited by mutations in the *CIF1*(*ACA10*) gene establishes a link between Ca^{2+} transport, vegetative phase change, and plant reproductive architecture. Further analysis of the interaction of the *CIF1* and *CIF2* gene, including identification of *CIF2* and characterization of its polymorphic alleles, will advance our understanding of this novel role for Ca^{2+} ion transport in plant development.

MATERIALS AND METHODS

Plant Materials, Growth Conditions, and Histochemical Assays

The Arabidopsis (*Arabidopsis thaliana*) *cif* mutant has been described (Goosey and Sharrock, 2001). The *psv* mutant was obtained from the Arabidopsis Biological Resource Center (The Ohio State University). Plants were grown under a 16-h photoperiod of fluorescent light at 21°C unless otherwise indicated. T-DNA insertion mutants in Arabidopsis Ws were identified in the *ACA8*, *ACA9*, and *ACA10* genes by PCR screening pools of insertion lines from the University of Wisconsin Arabidopsis knockout facility (Krysan et al., 1996). Two *aca8* lines (*aca8-1* = JHss106, with a kanamycin resistance marker; and *aca8-2* = JHss107, with a Basta-resistance marker), one

aca10 line (*aca10-1* = JHss110, with a kanamycin resistance marker), and the previously described *aca9-1* line (Schiott et al., 2004) were used. Plant lines homozygous for the T-DNA insertions were identified by the inability to amplify a wild-type band using primers from the respective genes flanking the inserts. T-DNA border fragments were amplified and sequenced for each insertion to verify the site of insertion. Histochemical GUS assays were performed as described (Goosey and Sharrock, 2001). Pollen staining was performed with malachite green-fuschin-orange G (Alexander, 1969).

Genetic Markers and Mapping

For mapping the *cif1-1* and *cif1-2* mutations, L*er*/Col simple sequence length polymorphism or insertion/deletion DNA markers from the Monsanto Arabidopsis Polymorphism and L*er* Sequence Collections (Jander et al., 2002) were screened to identify those that are also polymorphic between Col and the No-0 and/or S96 ecotypes. Supplemental Table S1 contains the sequences of PCR primers used to detect mutations and T-DNA insertions in various mutant lines. The *cif1-1* mutation was detected in crosses and transgenic lines by PCR amplification with primers LG593F and LG593R. The *aca10-1* T-DNA mutation was followed by PCR using a mixture of primers 346, 347, and 348. The *aca9-1* T-DNA mutation was followed by PCR using a mixture of primers 346, 349, and 350. The *aca8-2* T-DNA mutation was followed by PCR using a mixture of primers 346, 500, and 501. The $CIF2^{D:No\text{-}0}$ and $CIF2^{D:S96}$ alleles were distinguished from the $CIF2^{Col}$ and $CIF2^{Ws}$ alleles by assaying for a linked simple sequence length polymorphism marker, located on bacterial artificial chromosome F3C3, which was detected with primers LG231 and LG232.

Construction of *ACA8* and *ACA10* Transgenes and Plant Transformation

All *Agrobacterium* transformation plasmids were constructed as derivatives of pBI101.1 and confer kanamycin resistance (Jefferson et al., 1987). A 9.3-kb DNA fragment containing the wild-type allele of *ACA10*, extending from 1,460 bp upstream of the ATG to 275 bp downstream of the TAA stop codon, was PCR amplified from Col wild-type genomic DNA and cloned to create pBI-*ACA10*. To construct the P_{10}-10, P_{10}-8, P_8-10, and P_8-8 transgenes, the *ACA8* and *ACA10* coding regions, beginning at the start codons and including the introns, and the *ACA8* and *ACA10* promoter regions (2,700 bp and 1,460 bp) were PCR amplified from Col wild-type genomic DNA with restriction sites inserted at their ATG start codons. The various transgene fusion constructs were assembled and transformed into *cif1-1* host plants by the floral dip method (Clough and Bent, 1998). *ACA8*:GUS and *ACA10*:GUS transgenes were constructed by inserting the promoter fragments described above in front of the GUS coding sequence in the pBI101.1 vector. These GUS fusion genes were transformed into No-0 wild-type, Col wild-type, and *cif1-1* host plants by the floral dip method.

RNA Isolation, RNA Blots, and RT-PCR Analyses

Total RNA for northern-blot analysis was isolated from seven day-old light-grown seedlings, juvenile rosette leaves, and adult rosette leaves of No-0 wild-type and *cif1-1* plants as described (Clack et al., 1994). Poly(A)-enriched RNA was selected using an Oligotex Maxi kit (Qiagen). Hybridization probes were derived from nonconserved regions of the 5′ ends of the *ACA8* and *ACA10* cDNA sequences delimited by primer pairs 384/385 and LG592F/LG592R (Supplemental Table S1). Samples containing 1 μg of poly(A)-selected RNA were separated on agarose-formaldehyde gels, blotted, and hybridized as described (Clack et al., 1994). Total RNA for RT-PCR was isolated using an RNeasy kit (Qiagen). Samples containing 1.1 μg of total RNA were digested with RQ1 DNase I (Promega), and oligo(dT)-primed cDNA was synthesized using Superscript RNase H^- reverse transcriptase (Invitrogen). RT-PCR analysis of the *cif1-1* and *cif1-2* transcripts was performed with primer pairs LG589F/LG589R, which amplify from *ACA10* exon 28 to exon 30, and LG588F/LG588R, which amplify from *ACA10* exon 5 to exon 6. RT-PCR analysis of *ACA10* and *ACA8* transcript levels in T-DNA lines was performed using primer pairs LG589F/LG589R and 461/462, respectively. RT-PCR analysis of lines containing chimeric transgenes utilized primer sets that distinguish the wild-type *ACA10* and mutant *cif1-1* mRNAs (LG589F/LG589R), detect total *ACA8* mRNA (395/395), or detect only the mRNAs produced from the chimeric P_{10}-8 (412/413) or P_8-10 (579/580) transgene. Real-time qRT-PCR was performed in 25-μL reactions using 2× SYBR Green PCR master mix (Applied Biosystems) and a Rotorgene 3200 thermocycler (Corbett Life Science). Samples of cDNA were synthesized from total RNA as described above. Primer pairs q468/q469, q464/q465, and q551/q552 were used to quantify the *ACA8*, *ACA10*, and *UBQ10* cDNAs, respectively. The thermal profile was: 95°C for 10 min followed by 40 cycles of 95°C for 20 s, 55°C for 20 s, and 72°C for 20 s. Data were analyzed using Rotor-gene Version 5.0.61 software (Corbett Life Science). A relative calibrator standard curve was generated for each primer pair in each experiment from a control wild-type seedling cDNA sample. The expression level of the *ACA8* or *ACA10* transcript in each cDNA sample assayed was calculated based on the standard curve for that primer pair and was subsequently normalized to that of the control *UBQ10* transcript for that sample. Each experiment was repeated twice with independent biological samples and each sample was represented in triplicate in each experiment.

Phylogenetic Analysis

Protein sequences were aligned using Clustal (Chenna et al., 2003), and a branch and bound parsimony search was performed using PAUP* (Swofford, 2002). Bootstrap analysis implementing the branch and bound search option and a random addition of terminal taxa for each of 2,000 bootstrap replicates was performed.

Sequence data from this article can be found in the GenBank/EMBL data libraries under accession numbers NM_125093 (*ACA8*), NM_113013 (*ACA9*), and NM_119136 (*ACA10*).

Supplemental Data

The following materials are available in the online version of this article.

Supplemental Figure S1. Viability staining of pollen in the anthers of a *cif1/CIF1* heterozygous plant.

Supplemental Figure S2. Inflorescence phenotypes of the *aca* T-DNA mutants in the Ws ($CIF2^{Ws}$ recessive) background.

Supplemental Table S1. Oligonucleotide primers used in experiments.

ACKNOWLEDGMENTS

We thank the Arabidopsis Biological Resource Center (The Ohio State University) for providing genetic stocks and Mike Faul for technical assistance.

Received August 24, 2007; accepted December 3, 2007; published December 7, 2007.

LITERATURE CITED

Alexander MP (1969) Differential staining of aborted and nonaborted pollen. Stain Technol **44:** 117–122

Baxter I, Tchieu J, Sussman MR, Boutry M, Palmgren MG, Gribskov M, Harper JF, Axelsen KB (2003) Genomic comparison of P-type ATPase ion pumps in Arabidopsis and rice. Plant Physiol **132:** 618–628

Berridge MJ, Bootman MD, Roderick HL (2003) Calcium signalling: dynamics, homeostasis and remodelling. Nat Rev Mol Cell Biol **4:** 517–529

Bhatt AM, Etchells JP, Canales C, Lagodienko A, Dickinson H (2004) VAAMANA: a BEL1-like homeodomain protein, interacts with KNOX proteins BP and STM and regulates inflorescence stem growth in *Arabidopsis*. Gene **328:** 103–111

Bonza MC, Morandini P, Luoni L, Geisler M, Palmgren MG, De Michelis MI (2000) *At*-ACA8 encodes a plasma membrane-localized calcium-ATPase of Arabidopsis with a calmodulin-binding domain at the N terminus. Plant Physiol **123:** 1495–1506

Cerana M, Bonza MC, Harris R, Sanders D, De Michelis MI (2006) Abscisic acid stimulates the expression of two isoforms of plasma membrane Ca^{2+}-ATPase in *Arabidopsis thaliana* seedlings. Plant Biol (Stuttg) **8:** 572–578

Chenna R, Sugawara H, Koike T, Lopez R, Gibson TJ, Higgins DG, Thompson JD (2003) Multiple sequence alignment with the Clustal series of programs. Nucleic Acids Res **31:** 3497–3500

Clack T, Mathews S, Sharrock RA (1994) The phytochrome apoprotein family in Arabidopsis is encoded by five genes: the sequences and expression of *PHYD* and *PHYE*. Plant Mol Biol **25:** 413–427

Clough SJ, Bent AF (1998) Floral dip: a simplified method for *Agrobacterium*-mediated transformation of *Arabidopsis thaliana*. Plant J **16:** 735–743

Douglas SJ, Chuck G, Dengler RE, Pelecanda L, Riggs CD (2002) *KNAT1* and *ERECTA* regulate inflorescence architecture in *Arabidopsis*. Plant Cell **14:** 547–558

Evans NH, McAinsh MR, Hetherington AM (2001) Calcium oscillations in higher plants. Curr Opin Plant Biol **4:** 415–420

Geisler M, Frangne N, Gomes E, Martinoia E, Palmgren MG (2000) The *ACA4* gene of Arabidopsis encodes a vacuolar membrane calcium pump that improves salt tolerance in yeast. Plant Physiol **124:** 1814–1827

Goosey L, Sharrock R (2001) The *Arabidopsis compact inflorescence* genes: phase-specific growth regulation and the determination of inflorescence architecture. Plant J **26:** 549–559

Hanzawa Y, Takahashi T, Komeda Y (1997) *ACL5*: an *Arabidopsis* gene required for internodal elongation after flowering. Plant J **12:** 863–874

Hanzawa Y, Takahashi T, Michael AJ, Burtin D, Long D, Pineiro M, Coupland G, Komeda Y (2000) *ACAULIS5*, an *Arabidopsis* gene required for stem elongation, encodes a spermine synthase. EMBO J **19:** 4248–4256

Harper JF, Hong B, Hwang I, Guo HQ, Stoddard R, Huang JF, Palmgren MG, Sze H (1998) A novel calmodulin-regulated Ca^{2+}-ATPase (*ACA2*) from *Arabidopsis* with an N-terminal autoinhibitory domain. J Biol Chem **273:** 1099–1106

Hetherington AM, Brownlee C (2004) The generation of Ca^{2+} signals in plants. Annu Rev Plant Biol **55:** 401–427

Huang L, Berkelman T, Franklin AE, Hoffman NE (1993) Characterization of a gene encoding a Ca^{2+}-ATPase-like protein in the plastid envelope. Proc Natl Acad Sci USA **90:** 10066–10070

Hunter C, Willmann MR, Wu G, Yoshikawa M, de la Luz Gutierrez-Nava M, Poethig SR (2006) Trans-acting siRNA-mediated repression of ETTIN and ARF4 regulates heteroblasty in *Arabidopsis*. Development **133:** 2973–2981

Hwang I, Harper JF, Liang F, Sze H (2000a) Calmodulin activation of an endoplasmic reticulum-located calcium pump involves an interaction with the N-terminal autoinhibitory domain. Plant Physiol **122:** 157–168

Hwang I, Sze H, Harper JF (2000b) A calcium-dependent protein kinase can inhibit a calmodulin-stimulated Ca^{2+} pump (ACA2) located in the endoplasmic reticulum of *Arabidopsis*. Proc Natl Acad Sci USA **97:** 6224–6229

Jander G, Norris SR, Rounsley SD, Bush DF, Levin IM, Last RL (2002) Arabidopsis map-based cloning in the post-genome era. Plant Physiol **129:** 440–450

Jefferson RA, Kavanaugh TA, Bevan MW (1987) GUS fusions: B-glucuronidase as a sensitive and versatile gene fusion marker in higher plants. EMBO J **6:** 3901–3907

Kanrar S, Onguka O, Smith HM (2006) *Arabidopsis* inflorescence architecture requires the activities of KNOX-BELL homeodomain heterodimers. Planta **224:** 1163–1173

Krysan PJ, Young JC, Tax F, Sussman MR (1996) Identification of transferred DNA insertions within *Arabidopsis* genes involved in signal transduction and ion transport. Proc Natl Acad Sci USA **93:** 8145–8150

McSteen P, Leyser O (2005) Shoot branching. Annu Rev Plant Biol **56:** 353–374

Poethig RS (2003) Phase change and the regulation of developmental timing in plants. Science **301:** 334–336

Relichova J (1976) Some new mutants. Arabidopsis Inf Serv **13:** 25–28

Sanders D, Pelloux J, Brownlee C, Harper JF (2002) Calcium at the crossroads of signaling. Plant Cell (Suppl) **14:** S401–S417

Schiott M, Romanowsky SM, Baekgaard L, Jakobsen MK, Palmgren MG, Harper JF (2004) A plant plasma membrane Ca^{2+} pump is required for normal pollen tube growth and fertilization. Proc Natl Acad Sci USA **101:** 9502–9507

Shpak ED, Berthiaume CT, Hill EJ, Torii KU (2004) Synergistic interaction of three ERECTA-family receptor-like kinases controls *Arabidopsis* organ growth and flower development by promoting cell proliferation. Development **131:** 1491–1501

Smith HM, Hake S (2003) The interaction of two homeobox genes, *BREVIPEDICELLUS* and *PENNYWISE*, regulates internode patterning in the *Arabidopsis* inflorescence. Plant Cell **15:** 1717–1727

Strehler EE, Zacharias DA (2001) Role of alternative splicing in generating isoform diversity among plasma membrane calcium pumps. Physiol Rev **81:** 21–50

Sussex IM, Kerk NM (2001) The evolution of plant architecture. Curr Opin Plant Biol **4:** 33–37

Swofford D (2002) PAUP*. Phylogenetic Analysis Using Parsimony (*and Other Methods), Version 4.0 beta 10. Sinauer Associates, Sunderland, MA

Telfer A, Bollman KM, Poethig RS (1997) Phase change and the regulation of trichome distribution in *Arabidopsis thaliana*. Development **124:** 645–654

Torii KU, Mitsukawa N, Oosumi T, Matsuura Y, Yokoyama R, Whittier RF, Komeda Y (1996) The *Arabidopsis ERECTA* gene encodes a putative receptor protein kinase with extracellular leucine-rich repeats. Plant Cell **8:** 735–746

Venglat SP, Dumonceaux T, Rozwadowski K, Parnell L, Babic V, Keller W, Martienssen R, Selvaraj G, Datla R (2002) The homeobox gene *BREVIPEDICELLUS* is a key regulator of inflorescence architecture in *Arabidopsis*. Proc Natl Acad Sci USA **99:** 4730–4735

Weberling F (1989) Morphology of Flowers and Inflorescences. Cambridge University Press, Cambridge, UK

White PJ, Broadley MR (2003) Calcium in plants. Ann Bot (Lond) **92:** 487–511

Wu G, Poethig RS (2006) Temporal regulation of shoot development in Arabidopsis thaliana by miR156 and its target SPL3. Development **133:** 3539–3547

Yokoyama R, Takahashi T, Kato A, Torii KU, Komeda Y (1998) The Arabidopsis *ERECTA* gene is expressed in the shoot apical meristem and organ primordia. Plant J **15:** 301–310

Zylinska L, Kawecka I, Lachowicz L, Szemraj J (2002) The isoform- and location-dependence of the functioning of the plasma membrane calcium pump. Cell Mol Biol Lett **7:** 1037–1045